Available online at www.sciencedirect.com
SCIENCE DIRECT®
Carbon 44 (2006) 537–545
CARBON
www.elsevier.com/locate/carbon

Enhanced acidity and pH-dependent surface charge characterization of successively oxidized graphite oxides

Tamás Szabó [a], Etelka Tombácz [a], Erzsébet Illés [a], Imre Dékány [a,b,*]

[a] Department of Colloid Chemistry, University of Szeged, Aradi vértanúk tere 1, H-6720 Szeged, Hungary
[b] Nanostructured Materials Research Group of the Hungarian Academy of Sciences, Aradi vértanúk tere 1, H-6720 Szeged, Hungary

Received 12 May 2005; accepted 4 August 2005
Available online 23 September 2005

Abstract

This pH-potentiometric study explores the factors influencing the surface charge developed in aqueous dispersions of graphite oxide (GO) after a series of oxidation treatments. Surface charging curves demonstrate that lamellar surfaces of GO are negatively charged in the entire pH range studied. While these curves were found to be independent from the concentration of the GO suspensions, they were greatly affected by the solution conditions: increasing the pH and the ionic strength promotes the dissociation of acidic surface sites as weaker functional groups progressively participate in the ion exchange process, and the electrolyte provides an effective shielding for the surface charge. Surface densities of dissociated functional groups were determined by the proton binding isotherms and the specific surface areas of GO samples. BET surface areas provided irrationally high values for site densities, while surface areas calculated by geometrical considerations gave acceptable site densities. Formation of more and more oxygen-containing groups upon the subsequent oxidation steps, detected by IR spectroscopy and elemental analysis, resulted in the enhanced acidity of graphite oxide.
© 2005 Elsevier Ltd. All rights reserved.

Keywords: Graphite oxide; Adsorption; Functional groups; Interfacial properties

1. Introduction

Subjection of graphite to exhaustive oxidation under drastic conditions (e.g. $NaClO_3/HNO_3$) leads to its total molecular dissolution with ultimate products of mellitic acid and CO_2 [1]. In case the oxidation is terminated at less prolonged reaction times a graphite compound can be separated as an intermediate oxidation product that is referred to as graphite oxide (GO). It is a non-stoichiometric material in which the lamellar structure of graphite is conserved, but its polyaromatic character is lost due to chemisorption of different oxygen-containing functional groups (C–OH, COOH, etc.) [2–4]. The relative amount of these groups covalently attached to the carbon grid of trans linked cyclohexane chairs depends on the degree of oxidation [5].

The increasing interest for graphite oxide may be explained by the fact that invocation of chemical or electrochemical oxidation seems to be the only approach for the preparation of a kinetically stable colloidal dispersion of quasi two-dimensional carbonaceous sheets. Aqueous GO suspensions were used for making graphitic film in industrial scale [6–9], for depositing ultrathin self-assembled graphitic films [10,11] and their excellent swelling/exfoliation properties were exploited to make polymer nanocomposites of GO [12–14].

It was observed a long time ago by Clauss et al. [2] that GO can be disaggregated in dilute alkaline solutions, and the as-prepared stable suspension coagulates

* Corresponding author. Address: Department of Colloid Chemistry, University of Szeged, Aradi vértanúk tere 1, H-6720 Szeged, Hungary. Tel.: +36 62 544210; fax: +36 62 544042.
E-mail address: i.dekany@chem.u-szeged.hu (I. Dékány).

0008-6223/$ - see front matter © 2005 Elsevier Ltd. All rights reserved.
doi:10.1016/j.carbon.2005.08.005

instantly by acidification. This behavior implies that pH plays an important role in the exfoliation/restacking processes of GO lamellae. Extensive studies on the acid–base properties of diverse carbons are described in the literature [15–19], yet, only very limited work has been reported on the explanation and quantification of the above mentioned phenomena for graphite oxide. Mainly the classical approach of Boehm (based on back titration of excess amounts of acids and bases of different strength) was used for GO [2,20], while its direct titrations were limited to the determination of cation-exchange capacity (CEC) values from the inflection points of alkalimetric titration curves [21,22]. In addition, ionic strength dependence of the CEC has been disregarded at all.

However, precise knowledge of the surface charge properties is a necessary first step towards understanding many of the experimental observations concerning the colloidal stability, rheological, adsorption and electrokinetic properties, etc., of GO suspensions. These issues, along with the examples quoted above, point out that sophisticated characterization of the pH- and ionic strength dependent surface charge state of graphite oxide is a challenging scientific task with major practical implications. Earlier pH-potentiometric studies of our laboratory on various inorganic (metal oxides [23–25], clays [23], activated carbons [26,27]) and organic colloids (humic acids [25]) demonstrate the excellent suitability of this method for the quantitative description of the surface charge formation of these materials. The aim of this study is to extend this technique to graphite oxide as well. Acid–base titration is a powerful tool to the determination of surface excess amounts of protons or surface densities of charged functional groups that are essential for the description of colloidal stability of aqueous GO suspensions, but inaccessible with other methods.

2. Experimental section

2.1. Preparation of a graphite oxide series

Four samples of progressively oxidized graphite oxides were prepared from natural graphite flakes (Kropfmühl AG, Germany) based on Brodie's method [28]. Ten grams of graphite (99.98 wt% C, 250–500 μm fraction) and 85 g of $NaClO_3$ were mixed in a flask in an ice-bath. Sixty milliliter of fuming HNO_3 was then added dropwise. Another portion of acid (40 mL) was added after 16 h and the slurry was heated to 60 °C and kept for 8 h. Heating rate (1.5 °C/min) was controlled to avoid dangerous deflagration. The reaction was terminated by transferring the mixture into 1 L of distilled water. The suspension was washed with 5×200 mL of 3 M HCl solution and with a copious amount of distilled water until the supernatant had a specific conductivity of 10 μS/cm. The residual graphite oxide was decanted and dried. This first specimen of the graphite oxide series (GO-1) was oxidized forth (to GO-2) applying the same procedure, except a triple quantity (30 g) of GO-1 was used instead of graphite. Then, the whole oxidation procedure was repeated twice more in the same fashion to obtain the graphites with the highest degree of oxidation. The four samples will be denoted as GO-1, GO-2, GO-3 and GO-4 where 1–4 correspond to the number of subsequent oxidation steps.

2.2. Procedures

2.2.1. Potentiometric acid–base titrations

The pH-dependent surface charge was determined by potentiometric acid–base titration under CO_2-free atmosphere using 0.1 M of KOH, NaOH and HCl, and background electrolytes (KNO_3, NaCl) by which three ionic strength values (0.005, 0.05 and 0.5 M) were kept constant during the experiments. Before the titrations GO samples were ground and equilibrated with the electrolyte solutions, sonicated and prepurged with purified N_2. Equilibrium titration was performed by a home-made, computer-controlled titration system. The pH electrode of the potentiometer was activated and calibrated with three buffer solutions to check its Nernstian response. For maintaining quasi-equilibrium condition during the titration, a criterion for pH settling (pH change in time less than a preset value) was introduced: the next titrant portion (0.01–0.1 mL) was added if the criterion (0.03 pH/min) was fulfilled. The intervals between adding titrant doses were maximally 10 min, but in most cases less time was enough for the establishment of the equilibrium. Parallel to the suspension titrations, background electrolyte titrations were also performed to convert the electrode output to hydrogen ion concentration. The determination of the net proton surface excess amounts was based on the calculation of the material balance for H^+/OH^- ions, including the determination of their experimental activity coefficients. The net proton surface excess amount (or net proton consumption), Δn^σ is characteristic for the surface charging and is defined as the difference between H^+ ($n^\sigma_{H^+}$) and OH^- ($n^\sigma_{OH^-}$) surface excess amounts related to the unit mass of solid. The surface excess amount (n^σ_i) of a solute i can be determined from the initial ($c_{i,0}$) and the equilibrium concentration ($c_{i,e}$)

$$n^\sigma_i = \frac{V(c_{i,0} - c_{i,e})}{m} \quad (1)$$

where V is volume of the liquid phase and m is the mass of the adsorbent [29]. The values of ($n^\sigma_{H^+}$) and ($n^\sigma_{OH^-}$) were calculated at each point of the titration from the initial and equilibrium concentrations of the H^+ and OH^- ions using the actual activity coefficients deter-

mined from the corresponding background electrolyte titrations. It is noteworthy that this method is based on the determination of change in H^+/OH^- concentration in liquid phase due to interfacial protolytic processes, thus, any acid/base impurities of the titrated sample cause a mistake.

2.2.2. Additional characterization of GO

TEM images of GO-1 were taken with a Philips CM-10 electron microscope. Samples of sonicated suspensions (0.1 g/L) were dropped on copper grids coated by Formvar film. IR spectra were collected with a Biorad FTS-60A FT-IR instrument in diffuse reflectance mode. Elemental analysis was carried out by a Perkin-Elmer 2400 Series II. CHNS/O Analyzer. Specific surface area (a^S) was determined by N_2 adsorption using a Micrometrics Gemini II 2375 surface area apparatus. Analysis was performed on GO specimens freeze-dried from dilute (0.2 g/L) suspensions of pH = 9–11.

3. Results and discussion

3.1. Base induced delamination of graphite oxide

A dilute (0.1 g/L, pH = 4.5) aqueous suspension of GO-1 was examined visually and by means of electron microscopy. Although increased laser light scattering of the supernatant indicated the partial disaggregation of GO-1 to form a fine colloid, its coarse particles were still visible, settling down in a short time. The photograph of the suspension is presented in Fig. 1 (left image); a clear supernatant and a compact sediment was obtained after 1 day aging. Neither prolonged stirring, nor ultrasonic agitation could cleave the crude platelet aggregates. Added NaOH, however, caused rapid and spontaneous exfoliation, resulting in the formation of a stable suspension as seen obviously from its more intensive light scattering (right hand side photograph in Fig. 1; no sediment after aging for 1 day).

This phenomenon can also be observed by TEM. A typical image of the GO at pH = 4.5 (Fig. 2a) shows some coarse slabs as well as finer lamellae with micron-sized or smaller lateral dimensions, being characteristic for the polydisperse acidic suspension. Upon NaOH addition (pH = 10), only very thin carbon foils in random spatial arrangement and crumpled conformation were observed that is indicative of a delaminated GO structure (Fig. 2b).

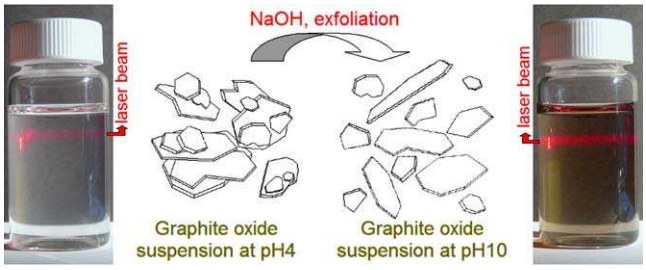

Fig. 1. Stability and laser light scattering of GO suspensions at pH = 4 and pH = 10.

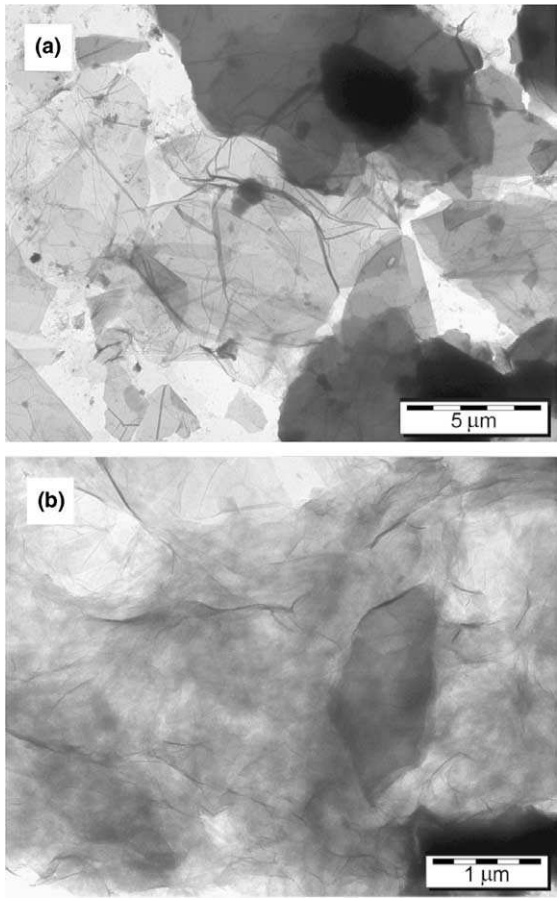

Fig. 2. TEM images of GO-1 suspension at pH = 4.5 (a) and at pH = 10 (b).

3.2. Origin of surface charge and the pH and ionic strength dependent colloid stability of GO

If graphite oxide is dispersed in aqueous medium, surface charge is generated on its platelets and at the edges by any surface sites or chemical groups that can undergo dissociation or are capable of ion adsorption from the solution. Taking into account the potential acid/base reactions of GO functional groups based on its structural models [2–5,20], the possible charging mechanisms of the GO surface are the following:

(i) deprotonation of carboxylic groups: $\rightarrow C\text{–}COOH + H_2O \iff \rightarrow C\text{–}COO^- + H_3O^+$,

(ii) deprotonation of enolic and phenolic groups: $>C{=}C^{\angle}OH + H_2O \iff >C{=}C^{\angle}O^- + H_3O^+$,

(iii) proton complexation of the π electron system of graphite planes acting as Lewis basic sites: $C_\pi + 2H_2O \iff C_\pi H_3O^+ + OH^-$, and
(iv) protonation of various Brönsted basic oxygen species (ethers, carbonyl groups).

The first two reactions afford negative surface charges, while (iii) and (iv) produce positive charges. Further investigations are needed to prove which of these reactions have chemical reality in the case of GO, i.e. whether these functionalities can be detected by any methods.

Graphite oxide consists of C, O and H atoms found by elemental analysis. Table 1 gives the empirical chemical formulae of the GO samples after taking into account the physically adsorbed water content determined from the difference between the masses of air-dry and anhydrous GO (samples dried over 96% H_2SO_4 for 1 month). Both oxygen and hydrogen content, along with the amount of H_2O, increase with the progressive oxidation treatment, indicating the formation of a hydrophilic graphite compound with more and more functional groups attached to the carbon skeleton. DRIFTS (Diffuse Reflectance FT-IR Spectroscopy) measurements substantiate these findings and provide some information on the evolution of the surface speciation of GO. While pristine graphite has a featureless spectrum (not shown), several characteristic peaks develop in the course of oxidation (Fig. 3). There is a collection of overlapping bands in the 3800–2200 cm^{-1} range of the spectra. They correspond to the O–H stretching vibrations of adsorbed water molecules and structural hydroxyl groups. Existence of more than two peaks suggests that OH groups are attached to the carbon layers in various forms, most probably as tertiary alcohols, enols, phenols, and COOH groups. The 1730 cm^{-1} band belongs to the C=O stretching vibration of COOH groups and/or ketones. Carboxylic and phenolic groups are located at the edges of the GO sheets [2], while the other species can be developed on the basal planes too. Finally, there is a band located near 1620 cm^{-1} that has a controversial assignment [30]. It can be attributed either to oxygen surface compounds, like cyclic ethers, or to the bending vibration of H_2O molecules. Moreover, ring vibrations of the basal plane appear very close, near 1590–1600 cm^{-1}. Since a shoulder at the lower frequency side of the peak can be identified for GO-1 (see the inset of Fig. 3), we assign the main peak to epoxide (cyclic 1,2-ether) groups and to the water content of GO, and the weaker, overlapping band at 1600 cm^{-1} to graphitic regions. In general, the intensities of all peaks increase from GO-1 to GO-4, especially that of C=O vibrations, in good agreement with the results of the water content and elementary analysis. On the contrary, the graphitic shoulder appears only in the spectrum of GO-1. The most important issues of the above experiments are that reactions (i)–(iv) are all potential charging reactions and that the amount of acidic groups increases, while that of the graphite regions decreases upon progressive oxidation.

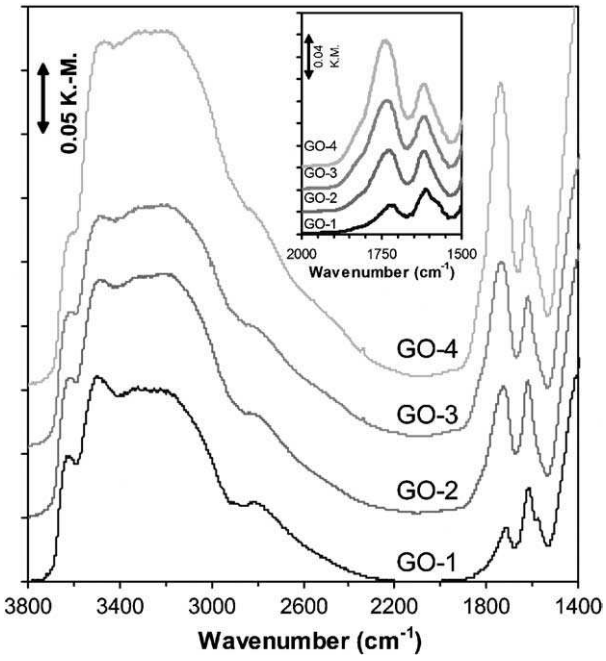

Fig. 3. DRIFT spectra of the graphite oxide samples.

It is evident that each of the above equilibrium reactions involves either H_3O^+ or OH^- ions. These ions are referred to as potential-determining ions in the literature since their concentration will directly determine the electric potential (ψ_0) and, indirectly, the charge density (σ_0) at the particle surface. At low potentials [31]

Table 1
Chemical formulae, intercalated H_2O content, and specific surface area (measured by N_2 adsorption and calculated in Appendix) of GO samples

Sample	Chemical formula	H_2O content (wt%)	a^S_{BET} (m^2/g)	a^S_{calc} (m^2/g)	Δn^σ (mmol/g)	Ξ ($1/nm^2$)	$\Xi/\Delta n^\sigma$ a.u.
GO-1	$CO_{0.39}H_{0.15}$	7.7	26	1807	−1.33	0.44	100
GO-2	$CO_{0.45}H_{0.17}$	10.0	40	1712	−1.85	0.65	106
GO-3	$CO_{0.46}H_{0.20}$	10.4	43	1695	−2.02	0.72	108
GO-4	$CO_{0.49}H_{0.20}$	11.2	30	1657	−2.33	0.85	110

Net proton surface excesses (Δn^σ) and surface densities of charged groups (Ξ) are compared at pH 10 and 0.005 M ionic strength.

$$\sigma_0 = \varepsilon\kappa\psi_0 \quad (2)$$

where ε is the permittivity, κ is linearly proportional to the ionic strength ($I = 1/2\,\Sigma c_i z_i^2$, c_i and z_i being the concentration and charge number of the ion i). For charged colloids like GO, the repulsive term of the total potential energy of interaction [32] between flat lamellar surfaces is due to the interaction between their electric double layer (EDL), which is influenced by both the I ionic strength and, through the ψ_0 surface potential, the pH. Now it is easy to understand why added electrolytes, acids and bases affect the surface charge and govern colloid stability.

3.3. Potentiometric acid–base titration of graphite oxides from subsequent oxidation steps

Initial pH-s of 0.1% suspensions of the graphite oxide series are plotted in Fig. 4. At each ionic strengths, there is a linear decrease of pH with the degree of oxidation. This indicates, in accordance with the DRIFT spectra, that the number of acidic surface sites linearly increases upon the number of oxidative treatments of graphite.

Cation-exchange capacities of graphite oxides are most commonly determined from the inflection points of titration curves [21,22]. To illustrate the influence of conditions under which the titration of GO is performed, and the ill-defined character of the titration curves, we show an example among our several titrations (GO-1 samples of 50 mg titrated with 0.1 M NaOH in NaCl solutions of different ionic strengths). As presented in Fig. 5, the waves of the titration curves, along with the positions of the inflection points, shifted towards higher titrant consumptions with increasing ionic strength. The question may arise which of these curves is the one characterizing the acid–base behavior of the sample and how to determine a titration endpoint for such featureless curves. We point out that acidity and cation exchange on GO cannot be characterized by a single value, since it is considered to be a

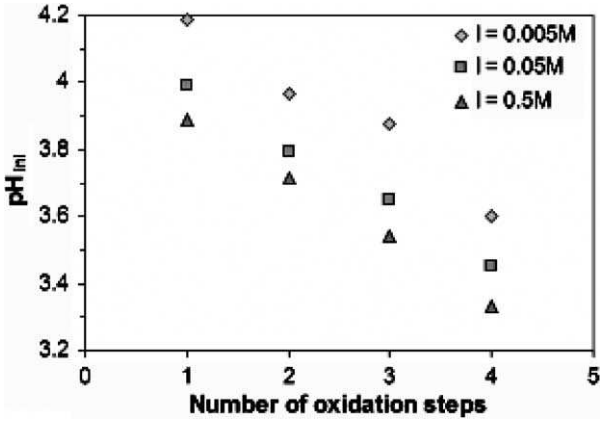

Fig. 4. Initial pH values of 0.1 g/100 cm^3 GO suspensions at different ionic strengths of the background NaCl.

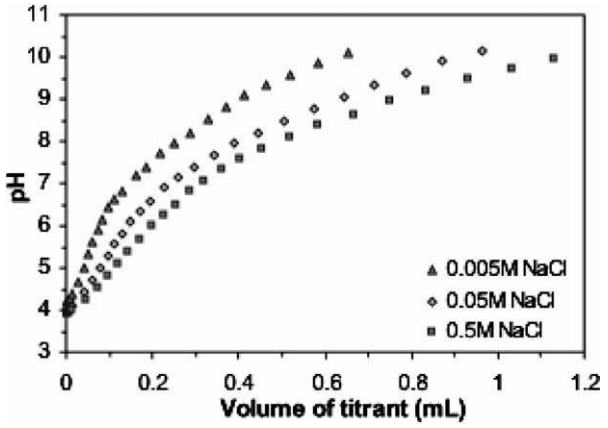

Fig. 5. Titration curves of GO-1 (50 mg) with 0.1 M NaOH at different ionic strengths.

weakly acidic cation exchanger [33], and thus its CEC depends on the pH and the salt concentration of the suspension. At high pHs and ionic strengths, though, there is a saturation for the CEC.

Three different weights of GO-1 (10 mg; 25 mg and 50 mg) were titrated with KOH in 50 mL of 0.05 M KNO_3. Although air-dry samples were used in all the experiments, Δn^{σ} values were calculated using the masses of the corresponding anhydrous graphite oxides. Δn^{σ} vs pH curves (also referred to as proton binding isotherms) are presented in Fig. 6. Negative Δn^{σ} values were measured in the entire pH range studied which indicates net base consumption, i.e. release of protons of the acidic sites, described by reactions (i) and (ii). This implies either the lack of polyaromatic regions in case of the highly oxidized samples (in accordance with the IR results) or that the number and extension of the graphitic islands and the amount of weakly basic oxygen species are too small to affect the interfacial protolytic processes even at the lowest pHs. Thus, reaction (iii) and (iv) has no significant contribution to surface charge.

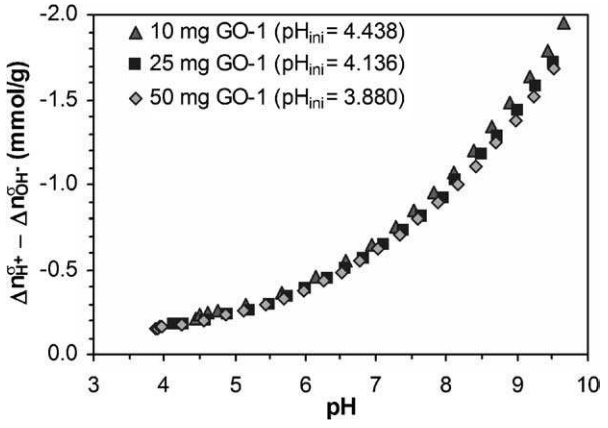

Fig. 6. pH-dependence of net proton surface excess amount of GO-1 at different suspension concentrations (0.05 M KNO_3 background electrolyte).

The inherent pHs of the GO-1 suspensions are around 4, and the Δn^{σ} values are very low. Since Δn^{σ} is linearly proportional to the surface density of charged species (Ξ), it is concluded that relatively few groups are deprotonated at this acidic pH. As the pH is increasing in the course of the titration, concentration of the protons in the liquid phase is decreasing due to the neutralization reaction with the added OH^- ions. Consequently, equilibrium reactions (i) and (ii) tend towards the right, generating more and more dissociated surface moieties as shown by the higher Δn^{σ} values. The proton binding curves do not exhibit distinctive inflection points, bending smoothly upwards instead. The reason is that the ionizable groups located in different parts of GO lamellae (e.g. enolic groups of basal planes, or COOH groups at the edges of the layers) are in different environments at molecular level, therefore the GO surface is inherently heterogeneous in a chemical point of view. Although the various acidic groups have different pK_a values, an overlapping of their broad pK_a distribution functions (due to the surface heterogeneity) is one of the probable reasons that no discrete inflection points appear on the surface charging curves [34,35]. Another plausible explanation is that the generated electrostatic field is homogeneous, since all the acidic groups are more or less randomly distributed on the carbon skeleton and hydration and ion adsorption smear out the electrostatic potential difference over the entire surface so the individual feature of surface sites vanishes [36]. The charge–potential curves obtained for the three different weights of GO-1 are essentially the same, except the initial pH-s are different (since the concentration of the "solid acid" GO is varying). At higher pH values, the small deviation for the smallest amount of GO titrated can be attributed to the increased error of mass measurement. The fact that the net proton surface excess amounts are independent of the suspension concentration means that potentiometric acid–base titration is suitable for the quantitative characterization of the acidity and provides a convenient measure for the pH-dependent surface charge state of GO.

Next, GO-1 suspensions of the same concentrations (50 mg sample in 50 mL solution) were titrated in two different background electrolytes (KNO_3 and NaCl) to study the influence of their chemical quality on surface charging. Ions near the interface of a charged colloid (i.e. in the electric double layer) are classified into two types in the literature: (a) ions of an indifferent electrolyte whose distribution in the EDL is only governed by the local electric field and the random thermal motion, and (b) specifically adsorbed ions that are strongly bound to the surface by any chemical interactions (or dimensional factors, such as the affinity of K^+ ions to montmorillonite). Potential specific ion adsorption could be observed by a difference in the initial pHs of suspensions containing the two types of ions. The reason is that if ions capable of specific interaction with the surface sites are present in the liquid phase, they will rapidly exchange the protons since they have higher affinity towards the surface and hence, a decrease in pH occurs. Fig. 7 shows the surface charging curves of GO-1 in both KNO_3 and NaCl of 0.5 M concentration; to avoid input of ions other than K^+ and Na^+, the titrants were KOH and NaOH, respectively. The proton binding isotherms run together and start from exactly the same pH (difference between them is 0.005 pH unit which is inside the error limits of pH and mass measurement). Thus, all of the studied ions (K^+, Na^+, Cl^- and NO_3^-) proved to be indifferent, forming just ion pairs with the charged sites.

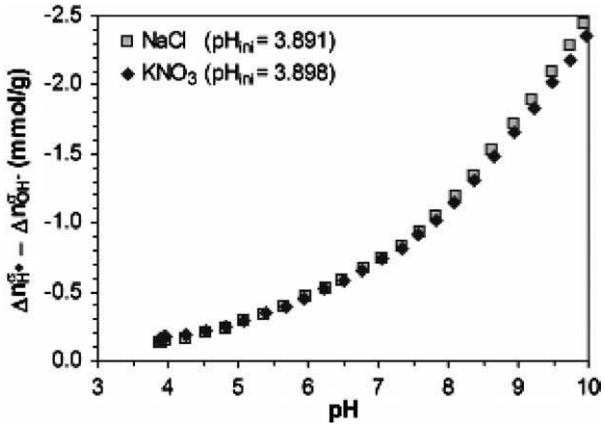

Fig. 7. Surface charging curves of GO-1 (0.1 g/100 cm^3 suspension) in different background electrolytes (KNO_3 and NaCl, $c = 0.5$ M).

The following experiments were performed with NaCl as background electrolyte and the titrant was NaOH. Each member of the GO series (50 mg) was titrated in NaCl solutions (50 mL) of three different ionic strengths. The surface charging curve of GO-1 is presented in Fig. 8 (curves of the other GO samples are not shown as they are very similar). Besides the conventional Δn^{σ} vs pH representation, surface density of charged species (Ξ) is also plotted on the right scale axis. Ξ (in 1/nm^2) can be calculated from Δn^{σ} (in mmol/g) by means of the specific surface area (a^S, m^2/g) and Avogadro's constant (N_A, 1/mol)

$$\Xi = -\frac{\Delta n^{\sigma} N_A}{10^{21} a^S} \tag{3}$$

Specific surface areas of freeze-dried GO samples determined by N_2 adsorption are collected in Table 1. Substitution of these values into (3) gives Ξ as high as 76/nm^2 in case of GO-4 (pH = 10, in 0.5 M NaCl). This value is totally unrealistic: according to our calculation (in the Appendix), the hypothetic maximum amount of OH groups of GO surfaces is 18/nm^2. But even this number is too high, since it is hard to imagine that such a high number of surface species could be dissociated, generating a tremendously high surface potential. Thus, we have reconsidered the validity of the BET surface

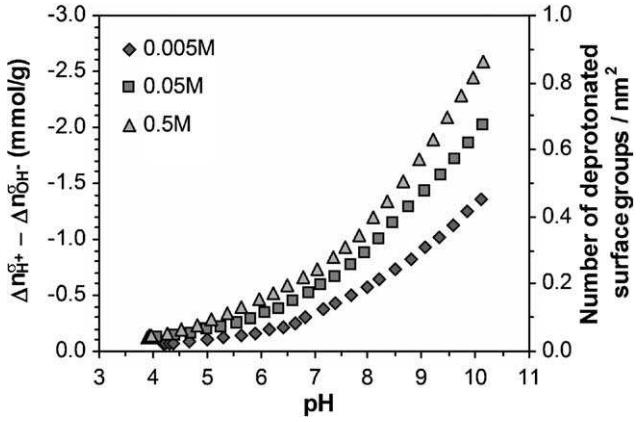

Fig. 8. Proton binding isotherms of the GO-1 at different NaCl concentrations. Surface densities of charged species (Ξ) are plotted in the right hand scale.

areas for the interpretation of our results (most probably nitrogen molecules cannot penetrate into the interlamellar space of freeze-dried graphite oxide), and came to the conclusion that the acid–base processes in aqueous GO dispersions take place on much greater surfaces. Note that accessibility of water molecules and oxonium ions into the intergallery space of GO (therefore, to the total surface) is an experimental fact substantiated by numerous XRD measurements [2,37,38]. Geometrical considerations of the structure of graphite oxide (detailed in the Appendix) led us to give calculated specific surface areas for the GO series (Table 1). These values agree very well with that (1760 m^2/g) found by the analysis of liquid (ethanol/cyclohexane) sorption isotherms of GO [37,39]. Application of these calculated specific surface areas in (3) produces densities in the Ξ range of 0.001–1.4 charged species/nm^2, which are in the same magnitude as reported by Clauss et al. [2] and Cassagneau et al. [21], although the way how they obtained their results is not detailed. We must also note here that Ξ refers only to a mean density of charged species on the surface, which is proportional to the surface charge density, assuming a homogeneous spatial distribution of dissociated surface sites.

For each sample, there is a marked difference between the proton binding isotherms: the higher the ionic strength is, the higher the Δn^{σ} and Ξ values are. The experimental fact that the measured charge–potential curves depend on the ionic strength provides a conclusive proof that the above reactions are exclusively responsible for the surface charge generation and base consumption, and no other reactions (e.g. neutralization of any acidic impurities) occur. It is explained in terms of Eq. (2): as the surface potential (ψ_0) is determined by the H^+/OH^- concentration (hence they are called potential-determining ions), it is constant at a given pH. Adding indifferent electrolyte (i.e. increasing the ionic strength) increases κ and results in a simultaneous increase of the surface charge density (σ_0, C/m^2, which is proportional to Ξ, $1/nm^2$) caused by the adsorption/desorption of sufficient H^+ ions to keep ψ_0 constant. In a practical point of view, we point out that the cation exchange capacity of GO can be increased only by adding indifferent salts to the solution; it may be beneficial in such cases when high pH should be avoided (e.g. ion-exchange with metal ions/complexes that readily hydrolyze).

Fig. 9 shows the surface charging curves of the GO series in 0.005 M NaCl. As expected, there are significant differences between them. The initial pHs are lower while the corresponding proton surface excess amounts are higher for the most oxidized graphites (Δn^{σ} and Ξ for each specimens at pH = 10 and the smallest ionic strength are compared in Table 1). These values are essentially lower than those obtained from the classical Boehm titration results by Scholz and Boehm [20]. This apparent contradiction can be explained by the fact that the tabulated Δn^{σ} and Ξ values are collected at pH = 10, so the solution conditions (pH and ionic strength) are not the same as in the Boehm titrations (0.1–2 M NaOH), in which, as a consequence of the higher pH, and the high ionic strength, much more acidic surface groups are evidently measured. The gradient of the curves in the acidic region also increases with the progressive oxidation. All these are in consistency with the infrared and elemental analysis results, pointing out that more and more acidic sites develop in the course of the oxidative treatment of graphite. The splitting of the curves are more pronounced if Ξ is plotted against the pH (not shown), because the differences between the specific surface areas cause higher deviations in the charged site densities calculated by (3). This can

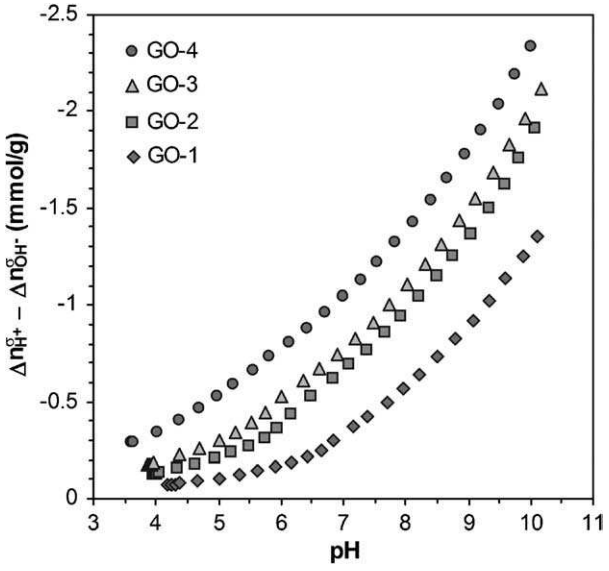

Fig. 9. pH-dependence of net proton surface excess amounts of the GO series at $c_{NaCl} = 0.005$ M.

be clearly seen from the increase of $\Xi/\Delta n^{\sigma}$ (its values in arbitrary units, which are proportional to the reciprocal of the calculated surface area, are in Table 1).

Finally, it is worth focusing again in Fig. 4 showing the initial pH-s of the suspensions as a function of the number of oxidation steps. As mentioned before, prolonged oxidation affords higher acidic strengths for the graphite oxides, resulting in a nearly linear decrease of pH. The other important feature is that increasing ionic strength causes a concomitant decrease of pH. It can be explained by the well known charge screening effect of electrolytes [40]: the separation of each subsequent proton from the graphite oxide surface is resisted by the electric field created by the species which are already ionized. Increasing amount of added electrolyte, however, provides more and more effective shielding of charged surface, which allows the dissociation of further protons.

4. Conclusion

The present work provides evidence that potentiometric acid–base titration can be applied for the quantitative characterization of the pH-dependent charge formation on graphite oxide surfaces. Proton binding isotherms, along with infrared spectroscopic evidence, reveal that in the studied pH range the surface charge development on GO occurs in two equilibrium reactions: dissociation of (i) COOH and (ii) enolic and phenolic groups. The so called surface heterogeneity, along with the polyfunctional nature of graphite oxide, results in the overlap of individual functional group pK_a values and the lack of well-defined inflection points on the proton binding isotherms. Ions of KNO_3 and NaCl were found to be indifferent, playing no specific interaction with the functional groups of GO. Titration results have also shown that acidities of the graphite oxides increase with the progressive oxidation. Particular attention was paid for the pH and ionic strength dependence of the net proton surface excess amounts of graphite oxide: higher densities of deprotonated surface sites (found in the alkaline region at higher salt concentrations) are explained by the influence of the decreasing H^+ concentration on the interfacial acid–base reactions and the charge-screening effect of background electrolytes, respectively. These issues point out that ion-exchange on GO surfaces cannot be characterized by a single value of cation-exchange capacity, since it highly depends on the solution conditions, i.e. the pH and ionic strength. Boehm's method proves to be very useful for the quantification and comparison of the acid–base properties of activated carbons and graphite oxides, but it provides information on the surface acidity at certain, often very high pHs. Thus, neglecting the major influence of the above mentioned factors in any studies (e.g. adsorption from solutions) in which ion-exchange of graphite oxide is relevant may cause serious ambiguities at the interpretation of the experimental data or lead to false conclusions. Although all of these problems have been overcome by means of the delicate evaluation of the titration data, we are planning additional experiments to combine these results with those of streaming and ζ-potential measurements and pH-static investigations.

Acknowledgements

This work was supported by the Hungarian National Scientific Fund OTKA T034430 and OTKA M045609. The authors are grateful to Professor Hanns-Peter Boehm for his valuable remarks and for revising and improving the manuscript.

Appendix

Specific surface areas and maximum surface density of OH groups were calculated on the basis of the chemical formulae of graphite oxide and the geometrical parameters of its structural model proposed by Ruess [41]. According to the Ruess model, graphite oxide consists of wrinkled carbon sheets composed of trans linked cyclohexane chairs, and the fourth valencies of the carbon atoms are bound to axial OH-groups and ether oxygen atoms in 1,3-positions.

The projected area of a cyclohexane chair is hexagonal. It can be considered as a unit cell for the calculations since it is the simplest repeating unit of the carbon skeleton The side length (a) of one hexagon is 0.1456 nm, considering the C–C bond distance (0.1545 nm) and the angle of inclination between the plane assigned to two parallel bond axes and the equatorial plane of the cyclohexane ring (19.5°). Therefore, the surface area of one hexagon (s_{hex}) is

$$s_{hex} = \frac{6\sqrt{3}a^2}{4} \tag{4}$$

which is 0.05508 nm^2, but it has to be doubled since the carbon plane has two sides, so the total surface of a unit cell is 0.11016 nm^2. The mass of the unit cell needs to be calculated next. Each cyclohexane unit possesses six carbon atoms, but all of them belong to two other rings, so two carbon atoms are attributed to an individual unit cell. For the subsequently oxidized graphite oxides, contributions of heteroatoms (in this case oxygen and hydrogen) can be taken into account by the corresponding chemical formulae. According to these, masses of the unit cells are 6.09×10^{-23}, 6.43×10^{-23}, 6.49×10^{-23} and 6.64×10^{-23} g for GO-1, GO-2, GO-3 and GO-4, respectively. Finally, specific surface area of the

unit cell (which equals to that of the bulk substances, Table 1) is obtained by division of its total surface (0.11016 nm^2) by these mass values.

The maximum surface density of OH groups can be calculated assuming that only OH groups are bound to the basal planes of the carbon layers (no unoxidized, graphitic regions or other functional groups are present; note that COOH groups are located at the edges of the GO sheets). In this case, since 2 OH groups belong to each of the cyclohexane rings (having 0.11016 nm^2 surface area), a 1 nm^2 surface contains 18 OH groups. Thus, if all of these species were deprotonated, $\Xi = 18/nm^2$ would be obtained.

References

[1] Ubbeholde AR, Lewis FA. Graphite and its crystal compounds. Oxford: Oxford at the Clarendon Press; 1960. p. 110–1.

[2] Clauss A, Plass R, Boehm HP, Hofmann U. Untersuchungen zur Struktur des Graphitoxyds. Z anorg allgem Chem 1957;291:205–20.

[3] Nakajima T, Matsuo Y. Formation process and structure of graphite oxide. Carbon 1994;32:469–75.

[4] Lerf A, He H, Riedl T, Forster M, Klinowski J. ^{13}C and ^{1}H MAS NMR studies of graphite oxide and its chemically modified derivatives. Solid State Ionics 1997;101–103:857–62.

[5] Lerf A, He H, Forster M, Klinowski J. Structure of graphite oxide revisited. J Phys Chem B 1998;102:4477–82.

[6] Clauss A, Hofmann U. Determination of partial vapor pressure (of water) with graphite oxide membranes. Angew Chem 1956;68:522.

[7] Clauss A, Hofmann U, Weiss A. Membrane potentials on graphite oxide foils. Ber Bunsenges Phys Chem 1957;61:1284–90.

[8] Boehm HP, Clauss A, Hofmann U. Graphite oxide and its membrane properties. J Chimie Physique 1961;58:141–7.

[9] Maire J, Colas H, Maillard P. Membranes de carbone et de graphite et leurs proprietés. Carbon 1968;6:555–60.

[10] Kotov NA, Dékány I, Fendler JH. Ultrathin graphite oxide-polyelectrolyte composites prepared by self-assembly: transition between conductive and non-conductive states. Adv Mater 1996;8:637–41.

[11] Szabó T, Szeri A, Dékány I. Composite graphitic nanolayers prepared by self-assembly between finely dispersed graphite oxide and a cationic polymer. Carbon 2005;43:87–94.

[12] Matsuo Y, Tahara K, Sugie Y. Structure and thermal properties of poly(ethylene oxide)-intercalated graphite oxide. Carbon 1997;35:113–20.

[13] Liu P, Gong K, Xiao P, Xiao M. Preparation and characterization of poly(vinyl acetate)-intercalated graphite oxide nanocomposite. J Mater Chem 2000;10:933–5.

[14] Uhl FM, Wilkie CA. Preparation of nanocomposites from styrene and modified graphite oxides. Polym Degrad Stabil 2004;84:215–26.

[15] Boehm HP, Diehl E, Heck W, Sappok R. Surface oxides of carbon. Angew Chem 1964;76:742–51.

[16] Boehm HP. Surface oxides on carbon and their analysis: a critical assessment. Carbon 2002;40:145–9.

[17] Biniak S, Szymański G, Siedlewski J, Świątkowski A. The characterization of activated carbons with oxygen and nitrogen surface groups. Carbon 1997;35:1799–810.

[18] El-Sayed Y, Bandosz TJ. Adsorption of valeric acid from aqueous solution onto activated carbons: role of surface basic sites. J Colloid Interface Sci 2004;273:64–72.

[19] Contescu A, Vass M, Contescu C, Putyera K, Schwarz JA. Acid buffering capacity of basic carbons revealed by their continous pK distribution. Carbon 1998;36:247–58.

[20] Scholz W, Boehm HP. Betrachtungen zur Struktur des Graphitoxids. Z anorg allgem Chem 1969;369:327–40.

[21] Cassagneau T, Guérin F, Fendler JH. Preparation and characterization of ultrathin films layer-by-layer self-assembled from graphite oxide nanoplatelets and polymers. Langmuir 2000;16:7318–24.

[22] Liu ZH, Wang ZM, Yang X, Ooi K. Intercalation of organic ammonium ions into layered graphite oxide. Langmuir 2002;18:4926–32.

[23] Tombácz E, Csanaky C, Illés E. Polydisperse fractal aggregate formation in clay mineral and iron oxide suspensions, pH and ionic strength dependence. Colloid Polym Sci 2001;279:484–92.

[24] Tombácz E, Szekeres M. Interfacial acid–base reactions of aluminum oxide dispersed in aqueous electrolyte solutions 1. Potentiometric study on the dissolution of solid phase. Langmuir 2001;17:1411–9.

[25] Illés E, Tombácz E. The role of variable surface charge and surface complexation in the adsorption of humic acid on magnetite. Colloid Surf A 2003;230:99–109.

[26] László K, Tombácz E, Kerepesi P. Surface chemistry of nanoporous carbon and the effect of pH on adsorption from aqueous phenol and 2,3,4-trichlorophenol solutions. Colloid Surf A 2003;230:13–22.

[27] László K, Tombácz E, Josepovits K. Effect of activation on the surface chemistry of carbons from polymer precursors. Carbon 2001;39:1217–28.

[28] Brodie BC. Sur le poids atomique du graphite. Ann Chim Phys 1860;59:466–72.

[29] Everett DH. Basic principles of colloid science. London: Royal Society of Chemistry; 1988. p. 215–6.

[30] Fuente E, Menéndez JA, Díez MA, Suárez D, Montes-Morán MA. Infrared spectroscopy of carbon materials: a quantum chemical study of model compounds. J Phys Chem B 2003;107:6350–9.

[31] Shaw DJ. Introduction to colloid and surface chemistry. London-Boston: Butterworths; 1980. p. 150–5.

[32] Hunter RJ. Foundations of colloid science, vol. I. Oxford: Oxford at the Clarendon Press; 1991. p. 406–9.

[33] Maier V, Vesely J, Stulik K. Potentiometric response of some carbonaceous electrodes. J Electroanal Chem Interf Electrochem 1973;45:113–25.

[34] Strelko V, Malik DJ, Streat M. Characterisation of the surface of oxidized carbon adsorbents. Carbon 2002;40:95–104.

[35] Leon y Leon CA, Radovic LR. Interfacial chemistry and electrochemistry of carbon surfaces. In: thrower pa, editor. Chemistry and physics of carbon, vol. 24. New York: Dekker; 1994. p. 213–79.

[36] Koopal LK. Adsorption on new and modified inorganic sorbents. In: Dabrowski A, Tertykh VA, editors. Studies in surface science and catalysis, vol. 99. Amsterdam: Elsevier; 1996. p. 757–8.

[37] Dékány I, Krüger-Grasser R, Weiss A. Selective liquid sorption properties of hydrophobized graphite oxide nanostructures. Colloid Polym Sci 1998;276:570–6.

[38] Boehm HP, Clauss A, Fischer GO, Hofmann U. Das Adsorptionsverhalten sehr dünner Kohlenstoff-Folien. Z anorg allgem Chem 1962;316:119–27.

[39] Lopez-Gonzalez J de D, Martin-Rodriguez A, Monero-Castilla C, Rodriguez-Reinoso F. The adsorption of alcohols on several graphite oxides. Extended Abstracts and Program—12nd Biennial Conference on Carbon, Pittsburgh, PA; 1975. pp. 175–6.

[40] Tombácz E. Asorption from electrolyte solutions. In: Tóth J, editor. Adsorption: theory, modeling, and analysis; surfactant science series, vol. 107. Basel: Dekker; 2002. p. 711–42.

[41] Ruess G. Graphitic oxide. Monatsch Chem 1946;76:381–417.